Science of the Total Environment 628–629 (2018) 707–714

Contents lists available at ScienceDirect

Science of the Total Environment

journal homepage: www.elsevier.com/locate/scitotenv

Sunshine duration reconstruction in the southeastern Tibetan Plateau based on tree-ring width and its relationship to volcanic eruptions

Changfeng Sun [a], Yu Liu [a,b,c,*], Huiming Song [a], Qiufang Cai [a], Qiang Li [a], Lu Wang [a,d], Ruochen Mei [a,d], Congxi Fang [a,d]

[a] *The State Key Laboratory of Loess and Quaternary Geology, Institute of Earth Environment, Chinese Academy of Sciences, Xi'an 710061, China*
[b] *Interdisciplinary Research Center of Earth Science Frontier (IRCESF) and Joint Center for Global Change Studies (JCGCS), Beijing Normal University, Beijing 100875, China*
[c] *Open Studio for Oceanic-Continental Climate and Environment Changes, Qingdao National Laboratory for Marine Science and Technology, Qingdao 266237, China*
[d] *University of Chinese Academy of Sciences, Beijing 100049, China*

HIGHLIGHTS

- A 497-year sunshine duration was reconstructed in the southeastern Tibetan Plateau.
- Sunshine appeared a decreasing trend from the mid-19th to the early 21st centuries.
- Weak sunshine years matched well with years of major volcanic eruptions.
- Sunshine duration was possibly affected by large-scale climate forcing.

GRAPHICAL ABSTRACT

(a) The reconstructed monthly sunshine duration series from the prior September to the current June during 1517–2013 CE (gray line), an 11-year moving average (black line), the long-term mean (black horizontal line), and the mean value ± 1σ (gray horizontal lines); (b) 30-year (gray line) and 50-year (black line) running variance for reconstructed.

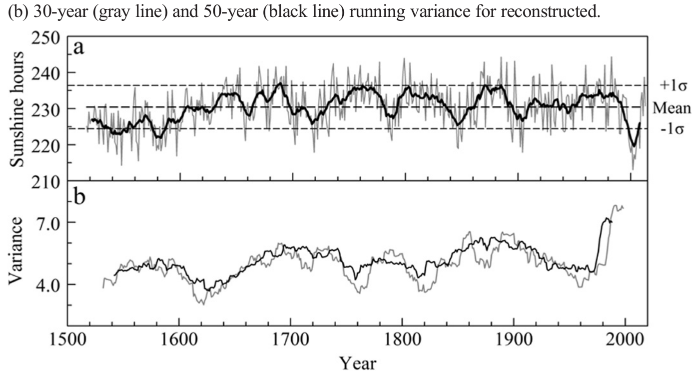

ARTICLE INFO

Article history:
Received 25 November 2017
Received in revised form 24 January 2018
Accepted 7 February 2018
Available online 20 February 2018

Editor: R. Ludwig

Keywords:
Sunshine duration
Reconstruction
Southeastern Tibetan Plateau
Tree-ring width
Volcanic eruption

ABSTRACT

Sunshine is as essential as temperature and precipitation for tree growth, but sunshine duration reconstructions based on tree rings have not yet been conducted in China. In this study, we presented a 497-year sunshine duration reconstruction for the southeastern Tibetan Plateau using a width chronology of *Abies forrestii* from the central Hengduan Mountains. The reconstruction accounted for 53.5% of the variance in the observed sunshine during the period of 1961–2013 based on a stable and reliable linear regression. This reconstructed sunshine duration contained six sunny periods (1630–1656, 1665–1697, 1731–1781, 1793–1836, 1862–1895 and 1910–1992) and seven cloudy periods (1522–1629, 1657–1664, 1698–1730, 1782–1792, 1837–1861, 1896–1909 and 1993–2008) at a low-frequency scale. There was an increasing trend from the 16th century to the late 18th and early 19th centuries and a decreasing trend from the mid-19th to the early 21st centuries. Sunshine displayed inverse patterns to the local Palmer drought severity index on a multidecadal scale, indicating that this region likely experienced droughts under more sunshine conditions. The decrease in sunshine particularly in recent decades was mainly due to increasing atmospheric anthropogenic aerosols. In terms of the interannual variations in sunshine, weak sunshine years matched well with years of major volcanic eruptions. The

* Corresponding author at: The State Key Laboratory of Loess and Quaternary Geology, Institute of Earth Environment, Chinese Academy of Sciences, Xi'an 710061, China.
E-mail address: liuyu@loess.llqg.ac.cn (Y. Liu).

https://doi.org/10.1016/j.scitotenv.2018.02.078

significant cycles of the 2- to 7-year, 20.0-year and 35.2-year durations as well as the 60.2-year and 78.7-year durations related to the El-Niño Southern Oscillation, the Pacific Decadal Oscillation and the Atlantic Multidecadal Oscillation suggested that the variation in sunshine duration in the southeastern Tibetan Plateau was possibly affected by large-scale ocean-atmosphere circulations.

1. Introduction

Tree rings, as a high-resolution climate proxy, have been widely employed in reconstructing past millennial and centennial climate changes and research areas ranged from single sites to regions to hemispheres and the whole globe (Esper et al., 2002; Mann et al., 2008; Popa and Kern, 2009; Pumijumnong and Eckstein, 2011; Griffin et al., 2013; Linderholm et al., 2015; Wilson et al., 2016). In China, dendroclimatology also has resulted in many important achievements through several decades of development, especially in recent years (Yang et al., 2014; Zhang et al., 2015; Liang et al., 2016; Liu et al., 2017a). Although studies of climate reconstructions have been conducted throughout the country (Zhang, 2015), the majority of these studies focus on precipitation, temperature, runoff and drought indexes (Shao et al., 2005; Liu et al., 2009, 2015, 2017b; Bao et al., 2012, 2015; Zhang et al., 2014; Chen et al., 2016). Based on our knowledge, no studies on sunshine reconstruction been conducted in China. Sunshine plays an equally important role as precipitation and temperature on tree grow in terms of photosynthesis and respiration. In addition, sunshine is tightly associated with moisture stress in trees. Therefore, the width of annual tree rings is under direct and indirect effects of sunshine duration (Poljansek et al., 2013). Under a suitable sunshine environment, the net photosynthetic rate of trees is relatively fast, and nutrient accumulation is greater; thus it is easier for trees to form wider rings. If sunshine is beyond the adaptive range of trees, either too much or too little, sunshine is not beneficial to carbohydrate synthesis and tree growth, and then, this can lead to narrower rings. Thus, tree rings can record past sunshine changes to some extent (Fritts, 1976). The first reconstructed sunshine duration was conducted for the central United State of America based on tree-ring width chronologies of bald cypress and post oak (Stahle et al., 1991). Using the tree-ring width of black pine, Poljansek et al. (2013) reconstructed summer sunshine for the period 1660–2010 for the western part of the Balkan Peninsula. In addition to tree-ring width, a stable carbon isotope was also utilized to perform a sunshine reconstruction (Gagen et al., 2011; Loader et al., 2013; Hafner et al., 2014). For example, Loader et al. (2013) provided a millennial-length reconstruction of summer sunshine for northern Sweden and indicated that the Arctic Oscillation could influence sunshine through cloud cover. However, these sunshine studies were from Europe and America, so it is necessary to fill the vacancy in sunshine reconstructions in China.

In addition, sunshine as the most direct indication of the performance of solar radiation is one of the important factors in climate formation (Yu et al., 2011). Sunshine is also a major driving element influencing the ecosystems of the earth and human activities; therefore, sunshine is being given more attention in climate change studies (Yang et al., 2012). However, studies related to sunshine in China have been based on meteorological data (Kaiser and Qian, 2002; Zheng et al., 2008; Yang et al., 2009; Xia, 2010; Li et al., 2011), and the instrumental record of sunshine is too short to fully understand the characteristics of sunshine and its potential driving factors.

Due to the many virgin forests and old trees in the middle section of the Hengduan Mountains, southeastern Tibetan Plateau, some past climate reconstructions have been conducted in these regions (Fan et al., 2008; Liang et al., 2009; Zhu et al., 2011; Shi et al., 2015). *Abies forrestii* as one dominant species of Hengduan Mountains has a wide altitude distribution, and its tree rings contain climate signals, such as precipitation and drought (Fang et al., 2010; Gou et al., 2013; Li et al., 2017). Studies have indicated that precipitation influences changes in sunshine, and droughts can be affected by sunshine through evapotranspiration (Thomas, 2000; Du et al., 2007; Yu et al., 2011; Yang et al., 2012). Therefore, while *Abies forrestii* can be used to reconstruct precipitation and drought, it likely contains sunshine signals as well. In this paper, we first utilized the tree-ring width of *Abies forrestii* to identify climate responses, and then, we reconstructed past sunshine for the southeastern Tibetan Plateau and finally discussed the effect of volcanic eruptions on sunshine.

2. Data and methods

2.1. The study area

The tree-ring sites are in Xiangcheng County of Sichuan Province in the Hengduan Mountains, southeastern Tibetan Plateau (Fig. 1). The climate is continental monsoon plateau, and a subtropical high pressure controls the regional climate change. Precipitation is mainly driven by the southwest monsoon, East Asian monsoon and plateau monsoon (Zhao and Chen, 1999).

According to the nearest meteorological station, Daocheng (approximately 36 km east of the tree-ring sites), the mean annual temperature is 4.5 °C, the annual precipitation 640.6 mm, and the annual sunshine duration is 2582.1 h (Fig. 2). High temperatures always occur in June–September, and precipitation is also mainly concentrated in these months, especially in July and August when 54.0% of the precipitation occurs. However, sunshine during these four months is less, and sunshine in July and August only accounts for 10.1%. Because of the large elevational range, the zones of mountainous area vegetation are clearly divided, and the forested zones appear at approximately 2400–4000 m. The main conifers in this area are *Abies*, *Tsuga* and *Picea* (Zhao and Chen, 1999).

2.2. Chronology and meteorology

Two groups of *Abies forrestii* tree-ring samples (Cook et al., 2010; Li et al., 2017) from Xiangcheng, Sichuan were used in this study (Table 1). Due to the close location of the two samples and their high environmental homogeneity, all the ring-width index series from the same species were merged to develop one chronology. To eliminate the non-climatic signals caused by the growth trend and other factors that influence width chronologies, negative exponential or linear curves of any slope were used to fit the growth trend. The detrended index series were merged to form a biweight robust mean chronology, with its variance stabilized by the Rbar weighted method (Osborn et al., 1997; Frank et al., 2007). Finally, the “signal-free” approach was used to mitigate potential trend distortion problems in the traditional chronology (Melvin and Briffa, 2008). The expressed population signal (EPS) can be used to evaluate the reliability of the tree-ring chronology (Wigley et al., 1984). In general, the greater the sample size is, the higher are the EPS values. An EPS value above 0.85 is generally regarded as satisfactory (Cook and Kairiukstis, 1990). In this research, an EPS value exceeding 0.85 existed after 1523 CE and corresponded to five cores from four trees. When the EPS decreased to 0.80, the chronology could extend to 517 CE with three cores from two trees.

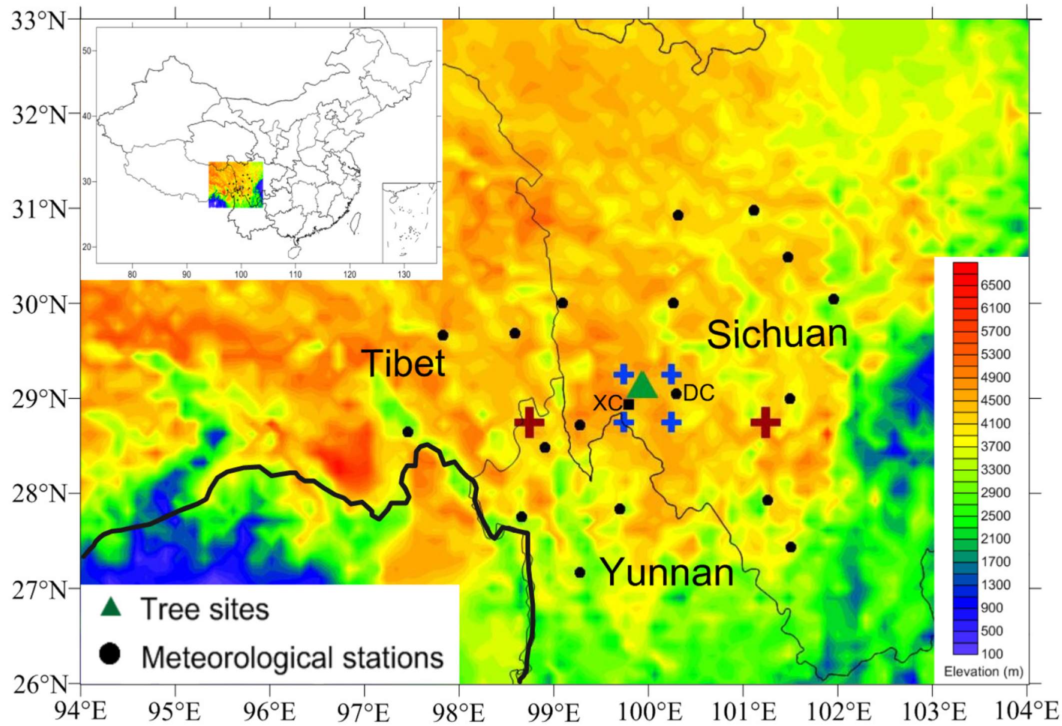

Fig. 1. Map of the location of the tree-ring sites (green triangle), meteorological stations (black circle), the four cloud cover grid points (blue cross) and the two PDSI grid points (red cross) used in this study. DC means Daocheng station, and XC is Xiangcheng County. (For interpretation of the references to colour in this figure legend, the reader is referred to the web version of this article.)

The meteorological data used in this study are mainly from Daocheng station (29.05°N, 100.30°E, 3727.7 m, 1961–2013 CE) that has the nearest distance to tree-ring sites. The climatic elements used in this study are temperature, precipitation and sunshine duration. From Fig. 2, we can see that in some months when there are higher temperatures and more precipitation, the sunshine duration is shorter. The data on sunshine duration from 18 stations within a 250-kilometer radius of the tree-ring sites were also used to conduct spatial representative analysis. Cloud cover data from the Climatic Research Unit (CRU) TS 3.24 (28.5–29.5°N, 99.5–100.5°E) covers the sites and Daocheng station, and the observed monthly Palmer drought severity index (PDSI) data of the two grids from the University Corporation for Atmospheric Research (UCAR) (28.75°N, 98.75°E and 28.75°N, 101.25°E) from 1961 to 2013 were also used. The two corresponding PDSI grid points in the Monsoon Asia Drought Atlas (MADA), a comprehensive gridded spatial reconstruction of Asian monsoon drought (Cook et al., 2010), were also utilized in this research. When studying the relation between sunshine and volcanic eruptions, the volcanic explosivity index (VEI) (Siebert and Simkin, 2013) that accurately records volcanic eruptions was employed. The VEI value for each volcanic event was obtained from http://volcano.si.edu.

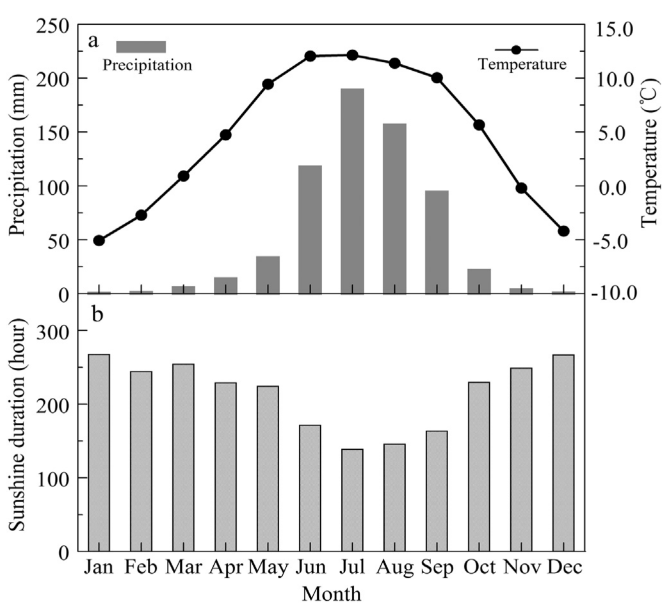

Fig. 2. Monthly mean temperature and total precipitation and sunshine duration at Daocheng meteorological station (1961–2013).

2.3. Statistical methods

In this study, Pearson's correlation analyses were used to identify climate-growth relationships between the tree-ring width indices and climate data during the observation period. Then, a simple linear regression model based on least squares was used for the sunshine reconstruction. The split calibration-verification procedure was used to verify the reconstruction function (Cook et al., 1999). The statistical parameters that provided for the calibration period were the Pearson's correlation coefficient(r) and the coefficient of determination (R^2), and the fidelity of the calibrations during the verification period was assessed via Pearson's correlation coefficient (r), the explained variance (r^2), the reduction of error (RE), the coefficient of efficiency (CE) and the sign test (ST). In general, the values of the most rigorous statistical analyses (RE and CE) are both positive, indicating a good model fit (Cook et al., 1999).

Table 1
The two tree-ring sites.

Site	Location	Elevation	Time span
Maxiong valley 01	29.15°N, 99.93°E	3530 m	1509–2006 CE
Maxiong valley 02	29.15°N, 99.95°E	3600 m	1498–2013 CE

The multi-taper method (MTM) of spectral analysis (Thomson, 1982) was used to detect the periodicities of the reconstructed sunshine. The ensemble empirical mode decomposition (EEMD) method (Wu et al., 2009), an adaptive and temporally local time series analysis method designed for analyzing non-linear and non-stationary climate data, was used to decompose the reconstructed sunshine series.

3. Results and discussion

3.1. Climate-growth relationship

Tree growth is affected not only by the climate of the current year but also the climate of the previous year (Fritts, 1976); therefore, correlation analysis between tree-ring chronology and major climatic variables (precipitation and mean temperature as well as sunshine duration) were performed from the previous June to the current September (Fig. 3). There were positive correlations between temperature and chronology, and statistically significant ($p < 0.05$) correlations were found from the previous November to the current April and current August. Positive correlations also occurred between precipitation and chronology with significant correlations ($p < 0.05$) at the previous September–October and current May–June. However, the relation between sunshine and chronology was negative, and the correlation coefficients passed a significant level ($p < 0.05$) in previous August–October and current May–June and August.

The response of precipitation and temperature to tree growth was similar to other studies in the southeastern Tibetan Plateau (Zhu et al., 2011; Gou et al., 2013; Li et al., 2017). In general, tree-ring width should be positively correlated with sunshine because sunshine mainly influences tree growth through photosynthesis. Photosynthesis in the tree canopy enhances with an increase in photosynthetically active radiation (PAR). However, photosynthesis is greater when the whole crown of a tree receives moderate PAR than when the upper canopy receives excessive PAR, and the lower canopy is in the shade (Farquhar and Roderick, 2003). The canopy with strong sun illumination is often light saturated and has low light-use efficiency (LUE) during sunny conditions, while the fraction in the shade has a higher LUE but much less PAR. In contrast, because the diffuse PAR coming from all directions of the sky can penetrate deeper into the canopy during cloudy conditions, it reduces the photosynthetic saturation and enhances the LUE of the whole canopy (Cho et al., 2003; Kanniah et al., 2012). Therefore, sunshine likely has a negative influence on tree growth for some species in some regions to a certain extent.

In addition, *Abies forrestii* is a shade-tolerant tree, so more sunshine is not beneficial to its growth. In addition, stronger sunshine could enhance transpiration and result in the loss of moisture. Stomata may close with increasing sunshine, which intensifies transpiration. Stomatal closure reduces photosynthesis and the accumulation of nutrients leading to narrower rings. Fritts (1976) found that the transpiration from shaded trees within a forest is often affected by variations in light, which affects stomatal opening and leaf resistance. Furthermore, the respiration of *Abies forrestii* is photorespiration with physical deterioration that is related to light. It was found that photorespiration in trees had high rates of net carbon dioxide production under high light levels during the day indicating high rates of respiration (Brown, 1968). This finding means that intense light accelerates respiration and can result in narrower rings.

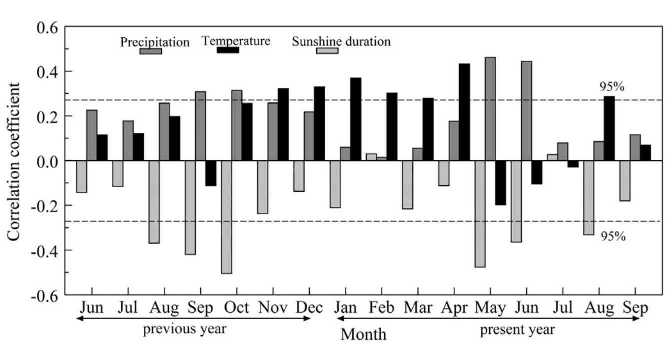

Fig. 3. Correlation between tree-ring chronology and climatic records during 1961–2013.

In summary, different species require different minimal light intensities to carry out photosynthesis, and they have different tolerances to light (Fritts, 1976). Intense solar radiation is related to reduced growth, probably due to various internal and external factors, such as increased leaf temperatures, higher respiration rates, consumption of stored photosynthesis, and accelerated evaporation of soil moisture, which may result in internal moisture stress and an overall reduction in the rates of photosynthesis and radial growth (Fritts, 1976). Under this situation, the width chronology of *Abies forrestii* has a negative relation with sunshine duration as the best indication of the performance of solar radiation (Fig. 3).

Generally, seasonal climate is more meaningful and stable than the climate of a single month. After combining the monthly data on all aspects of the climate conditions, the months with the highest correlations for the mean temperature were from the prior October to the current April ($r = 0.458$, $p < 0.01$). The highest correlation coefficient for precipitation occurred from the previous September to the current June ($r = 0.716$, $p < 0.01$), and the most significant correlation between sunshine and chronology also appeared from the previous September to the current June ($r = -0.731$, $p < 0.01$). In fact, the correlation for the temperature of the ten months was also significant ($r = 0.349$, $p < 0.01$). These results indicated that the climate of the previous September to the current June plays a more important role in tree growth. As stated previously, rainfall in July and August accounted for 54.0% of the annual precipitation; the high rainfall amounts could alleviate the moisture limitation for the trees; thus, there was a weaker relationship between the July–August rainfall and tree growth. The correlation coefficient between sunshine and chronology in August was −0.332 ($p < 0.05$), but the correlation between these two factors from the prior September to the current August ($r = -0.666$) was less significant. This result was likely because sunshine in July and August only accounted for 10.1% of the annual sunshine. At the same time, the partial correlations between the chronology and the previous September to the current June sunshine duration (SD_{96}) and the previous September to the current June precipitation (P_{96}) were calculated. The partial correlation between the chronology and SD_{96} when P_{96} was fixed was more significant ($r = -0.632$) than that between the chronology and P_{96} when SD_{96} was fixed ($r = 0.608$). Therefore, the width chronology of *Abies forrestii* can be used to reconstruct SD_{96}.

3.2. Transfer function and sunshine duration reconstruction

According to the abovementioned analyses, the mean SD_{96} was reconstructed from the tree-ring width chronology using the following linear regression model based on the least square method:

$$SD_{96} = -19.017^{*}\ W_t + 249.634$$

$$\left(n = 52, r = 0.731, R^2 = 53.5\%, R^2{}_{adj} = 52.5\%, F = 57.455, D/W = 1.83\right).$$

The Durbin-Watson statistic (D/W, (Durbin and Watson, 1950)) was used to detect the presence of autocorrelation in the residuals (when $n = 52$, a D/W value between 1.60 and 2.40 indicates that the reconstructed equation is free from first-order autocorrelations). From the function, it was found that the tree ring could explain 53.5% of the variations in sunshine duration.

The split calibration-verification method was used to test the stability and reliability of the transfer function (Cook et al., 1999). As shown in Table 2, the correlation coefficients between the observed and reconstructed data for all calibration and verification periods were significant at the 99% confidence level. The sign tests (ST) were significant at the 95% confidence level for most periods. The reduction of error (RE) and the coefficient of efficiency (CE) values for all verification periods were positive, indicating that the regression model had reasonable predictive capacity (Cook et al., 1999).

A visual comparison also showed that the reconstruction tracked the actual sunshine values well (Fig. 4a). After the first-order difference, there was still a significant correlation ($r = 0.587$, $p < 0.01$) between the two sequences (Fig. 4b), indicating that our reconstructed sequence captured the changes characteristic of the observed sequence at both high and low frequencies.

According to the length of the chronology, the monthly mean SD_{96} variations in the southeastern Tibetan Plateau for the period 1517 to 2013 were reconstructed using the above function (Fig. 5). During the past 497 years, the mean of SD_{96} was 230.4 h, and the standard deviation (σ) was 5.9 h. The multi-taper method spectral analysis showed that the reconstructed sunshine contained 2.3- to 7.7-year interannual cycles, 60.2-year and 78.7-year multidecadal cycles and 114-year centennial cycles at a 95% significant level. The series also had 12.6-year, 20.0-year and 35.2-year interdecadal periods at a 90% level (Fig. 6).

3.3. Characteristics of sunshine during the past 497 years

To investigate historical sunshine variations, we defined a more sunshine year as >mean + 1σ (236.3 h) and a less sunshine year as <mean − 1σ (224.5 h) (Fig. 5a). The full reconstruction of the sunshine displayed strong interannual variability from 1517 to 2013. During the past 497 years, 83 more sunshine years and 78 less sunshine years occurred in the reconstruction series, and they accounted for 16.7% and 15.7% of the total, respectively. In general, the long-lasting more or less sunshine events have much stronger effects on the local ecological environment and human activities. Then, we analyzed the multiyear continuous more or less sunshine years for the past 497 years based on the reconstruction. Longer sunshine events lasting over three years were found in 1670–1672, 1683–1686, 1765–1767, 1798–1800, 1867–1870 and 1936–1938. At the same time, long-lasting shorter sunshine durations were found in 1536–1538, 1542–1544, 1561–1563, 1579–1581, 1940–1942 and 1998–2006. It was easily found that the shorter sunshine durations mainly appeared in the 16th century and the end of the 20th century and the longer sunshine durations were in the 17–19th centuries.

To analyze the low-frequency variation of the reconstruction, an 11-year running average was applied (Fig. 5a). After smoothing, the entire reconstructed sunshine curve presented six sunny periods (1630–1656, 1665–1697, 1731–1781, 1793–1836, 1862–1895 and 1910–1992) with sunshine lasting a longer duration than the mean (230.4 h), and seven cloudy periods (1522–1629, 1657–1664, 1698–1730, 1782–1792, 1837–1861, 1896–1909 and 1993–2008) with sunshine lasting for a shorter duration than the mean. The longest cloudy epoch of 1522–1629 fell within the broad period described as the Little Ice Age (LIA). This result indicated that the short sunshine duration likely

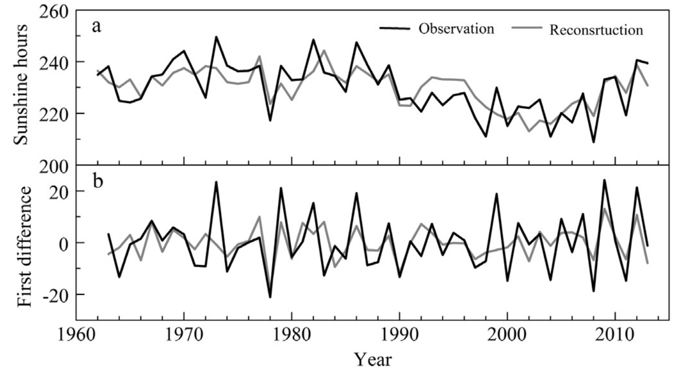

Fig. 4. (a) Comparison of reconstructed and observed mean sunshine durations from the prior September to the current June during the period 1962–2013 and (b) a comparison of their first-order differences.

resulted in low temperatures during the LIA. The cloudiest epoch appeared at the end of the 20th century and the beginning of the 21st century, and this result was likely associated with the increasing atmospheric anthropogenic aerosols that increased the aerosol extinction coefficient and decreased solar radiation and sunshine duration (Kaiser and Qian, 2002). It has been noted that, in China, increasing air pollution from human activities produced a fog-like haze that reflected and absorbed radiation from the sun, essentially reducing the amount of solar radiation reaching the earth's surface (Qian et al., 2006). Furthermore, several other studies have also found that increases in aerosols were the main driving force decreasing solar radiation and sunshine hours in some regions of China (Che et al., 2005; Qian et al., 2007). In addition, running variance analyses (Liu et al., 2017c) indicated that the variability in sunshine increased sharply and peaked after 1970 (Fig. 5b). This result might imply that the variation rule of sunshine in this region was altered owing to increasing human activities.

To present the variations in sunshine at different time scales, the reconstructed series was decomposed by using EEMD that could decompose sunshine into several intrinsic mode functions (IMFs) and a trend (Wu et al., 2009). From the results of the EEMD, we obtained the components of the reconstructed sunshine over the past 497 years (Fig. 7). The proportion of the total variance for each component was also calculated, and the results showed that the interannual component accounted for 39.6%, the interdecadal component accounted for 15.2%, the multidecadal component accounted for 20.6%, the centennial component accounted for 12.6%, and the long-term trend was 12.0%. A dominant feature of the record was shown in the trend change; there was an increase in sunshine from the 16th century to the late 18th and early 19th centuries. From the mid-19th century, a decrease appeared in the early 21st century. From the mid-19th century, gradually increasing human activities enhanced the emissions of aerosols leading to a reduction in solar radiation and sunshine. Some studies about decreasing

Table 2
Statistics of the split calibration-verification model for sunshine duration reconstruction.

Calibration				Verification					
Period	r	R^2	ST	Period	r	r^2	RE	CE	ST
1962–1993	0.599**	0.359	23*	1994–2013	0.658**	0.433	0.709	0.306	15*
1982–2013	0.738**	0.545	27**	1962–1981	0.561**	0.314	0.576	0.208	13
1962–2013	0.731**	0.535	42**						

r, correlation coefficient; RE, reduction of error test; CE, coefficient of efficiency; ST, sign test.
* Significant at the 95% level.
** Significant at the 99% level.

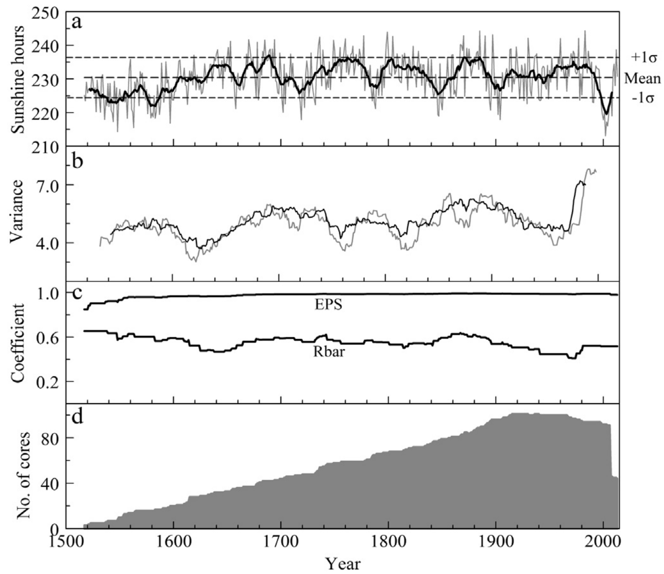

Fig. 5. (a) The reconstructed monthly sunshine duration series from the prior September to the current June during 1517–2013 CE (gray line), an 11-year moving average (black line), the long-term mean (black horizontal line), and the mean value ±1σ (gray horizontal lines); (b) 30-year (gray line) and 50-year (black line) running variance for reconstructed sunshine; (c) the running EPS and Rbar and (d) sample size.

solar radiation and sunshine at a global scale found that atmospheric anthropogenic aerosols and other pollutants were the major factors for "global dimming" (Stanhill and Cohen, 2001; Pinker et al., 2005).

3.4. Spatial representativeness and comparison with other reconstructions

The mean monthly sunshine at 18 stations within 250 km from the tree-ring sites were defined as the regional sunshine. The SD_{96} of Daocheng not only had a significant relation with the regional SD_{96} ($r = 0.652$, $p < 0.01$) during 1962–2013 but also the reconstructed SD_{96} significantly correlated with the regional SD_{96} ($r = 0.474$, $p < 0.01$). This result could indicate that the reconstructed SD_{96} was representative of the sunshine variations for a large region in the southeastern Tibetan Plateau to a certain extent.

In some regions, sunshine had an important relation with precipitation, which affected drought changes (Yang et al., 2009; Li et al., 2012b). In this region, we found that the observed SD_{96} significantly correlated with P_{96} ($r = -0.482$, $p < 0.01$) and that SD_{96} also had a significant relation ($r = -0.454$, $p < 0.01$, 1962–2013) with the PDSI of two grids from UCAR (28.75°N, 98.75°E and 28.75°N, 101.25°E), which covered the tree-ring sites and Daocheng station. This result showed that there was some relation between sunshine and drought in our study region. Thomas (2000) found that annual sunshine appeared to be the most important variable contributing to changes in potential evapotranspiration rates, which played an important role in drought changes.

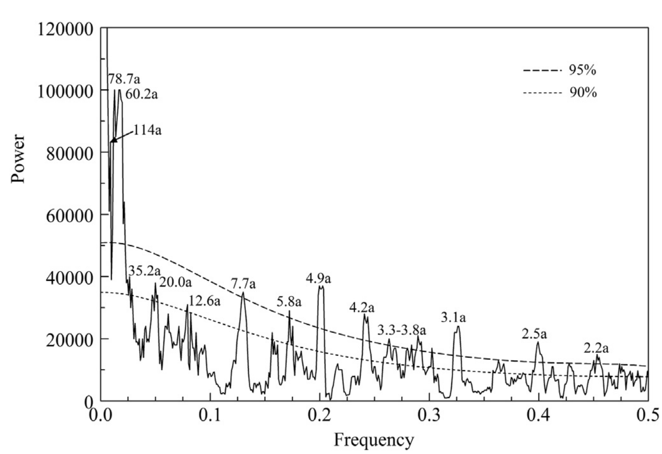

Fig. 6. Spectrum analysis result of the reconstructed sunshine duration (The long and short dashed lines indicate the 95% and 90% confidence levels, respectively).

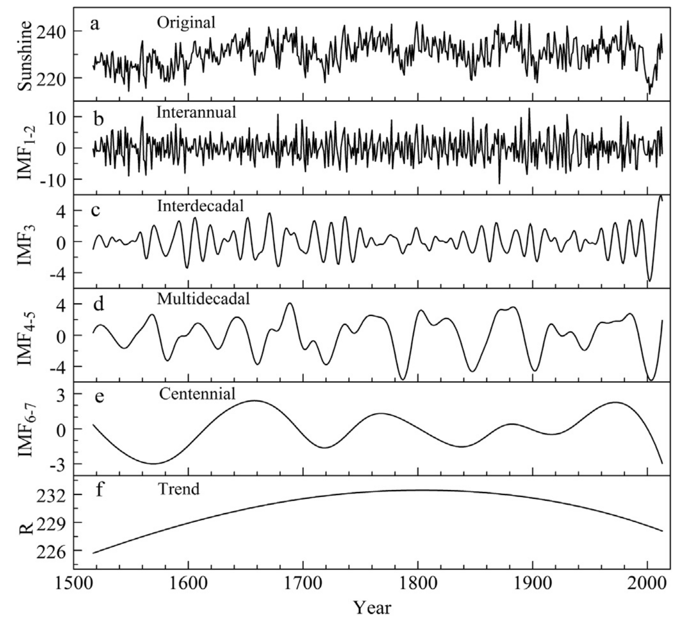

Fig. 7. IMFs of sunshine over the past 497 years based on the EEMD.

According to the above analysis and on the basis of the lack of reconstructed sunshine series, we conducted a comparison between our sunshine series and the reconstructed PDSI of MADA (Cook et al., 2010). The average of the two grids (28.75°N, 98.75°E and 28.75°N, 101.25°E) covering the sites and meteorological station was used. The correlation analysis showed that they had a significant relation ($r = -0.511$, $p < 0.01$, 1517–2005). Before conducting the comparison, the PDSI was also decomposed using the EEMD. It was found that there was negative phase relation for the sunshine series and the reconstructed PDSI at the multidecadal scale (Fig. 8). During the periods with more sunshine, the study region was likely to experience drought. This result could occur because more sunshine often occurred at the same time as less precipitation, and it also increased the evapotranspiration (Thomas, 2000).

3.5. Relationships between sunshine and volcanic eruptions

The previously mentioned increasing atmospheric anthropogenic aerosols were one of the many factors influencing sunshine changes. Similarly, atmospheric aerosols resulting from volcanic eruptions also affected sunshine variations. Pinker et al. (2005) attributed the possible causes of global dimming to increasing anthropogenic aerosols and the lowering of atmospheric transparency following explosive volcanic eruptions. The volcanic veil from strong eruptions could influence climate change through atmospheric propagation of radiation (Kelly et al., 1998).

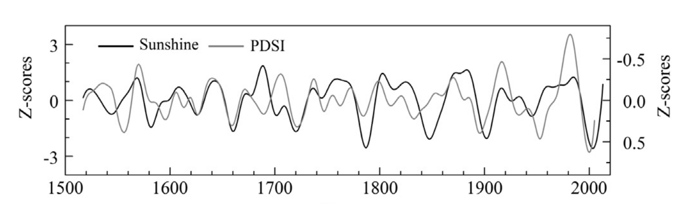

Fig. 8. Comparison between the reconstructed sunshine and the corresponding PDSI.

Large volcanic eruptions inject sulfur gases into the stratosphere, which are converted to sulfate aerosols with an e-folding residence timescale of several years (Robock, 2000). Therefore, the interannual series of the reconstructed sunshine (Fig. 7b) was used to study the relation between sunshine and volcanic eruptions. A weak sunshine year was defined as one year with sunshine less than the mean–1σ of the interannual series. To determine a major volcanic eruption, we employed a historical/geological record based on the VEI equal or greater than four. The comparison revealed that weak sunshine usually occurred the year after or the year of a large volcanic eruption over the past 497 years (Fig. 9), especially since the mid-18th century with more volcanic eruptions relative to before (Siebert and Simkin, 2013). There was no large volcanic eruption before or in 1871, which was the weakest sunshine year, but five volcanos (VEI = 3) erupted in 1870. The years with surprisingly low summer sunshine values in Bosnia and Herzegovina also matched well with the years of major volcanic eruptions over the past four hundred years (Poljansek et al., 2013).

Strong volcanic eruptions could send volcanic ash into the stratosphere with volcanic aerosols spreading to the world within a few months. The aerosols scattered some solar radiation and reflected some back to space, and then, the aerosols reduced the solar radiation reaching the ground and sunshine durations. It was found that volcanic activity was an important factor influencing the total decrease in solar radiation on the Tibetan Plateau during the past few decades, and sunshine change was affected by the solar radiation received on the surface (Li et al., 2012a; Yang et al., 2012).

3.6. Other influencing factors

It was found that cloud cover was an important factor influencing sunshine changes (Xia, 2010). The calculation results indicated the SD_{96} of Daocheng significantly correlated (r = –0.557, p < 0.01) with the cloud cover of the region around the sites from the CRU (28.5–29.5°N, 99.5–105.5°E). The negative correlation reflected the influence of cloud cover on sunshine hours because it can be weakened by increased cloudiness (Li et al., 2012b). Previously, we showed that SD_{96} showed a statistically significant negative correlation with precipitation. This corresponded to the fact that the frequent precipitation events had important influence on sunshine (Li et al., 2012b). It is well known that precipitation and cloud cover in this region are affected by the Asian monsoon, which is connected with the El-Niño Southern Oscillation (ENSO), the Pacific Decadal Oscillation (PDO) and the Atlantic Multidecadal Oscillation (AMO) (Mohtadi et al., 2016). In addition, the significant cycles of the 2- to 7-year fall within the range of variability of ENSO, the 20.0- and 35.2-year cycles are similar to the 20- to 30-year cycles of PDO, and the 60.2- and 78.7-year cycles correlate to the 60- to 80-year cycles of AMO. These results might suggest the influence of ENSO, PDO and AMO on sunshine changes in the southeastern Tibetan Plateau. Fang et al. (2010) found that drought in the southeastern Tibetan Plateau was linked to sea surface temperature variations in the northern Pacific and Atlantic Oceans. Of course, the specific relationships among them need further study and analysis.

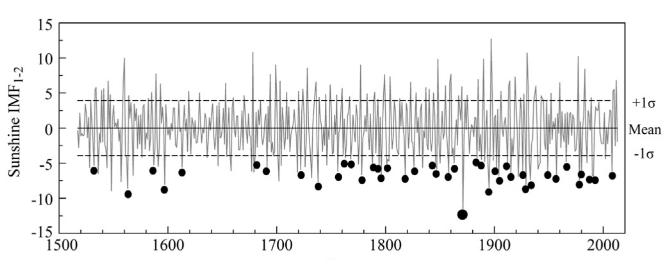

Fig. 9. Relationship between the interannual variations in the reconstructed sunshine and volcanic eruptions. The solid horizontal line represents the long-term mean of the interannual sunshine for the period of 1517–2013; the dashed horizontal lines represent the mean value ± 1σ. The solid cycles indicate a weak sunshine year following a volcanic eruption event.

4. Conclusions

The SD_{96} of the period 1517 to 2013 was reconstructed for the southeastern Tibetan Plateau using ring width of *Abies forrestii* from the middle section of the Henduan Mountains. The reconstruction accounted for 53.5% of the variance in the observed sunshine duration over the period of 1961–2013, and the transfer function was verified as stable and reliable. During the past 497 years, there were six sunny periods (1630–1656, 1665–1697, 1731–1781, 1793–1836, 1862–1895 and 1910–1992) and seven cloudy periods (1522–1629, 1657–1664, 1698–1730, 1782–1792, 1837–1861, 1896–1909 and 1993–2008) at a low frequency scale. An increasing trend appeared from the 16th century to the late 18th and early 19th centuries, followed by a decreasing trend in the early 21st century. It was found that the reconstructed sunshine durations compared well with the regional PDSI, and this region likely experienced drought under longer sunshine conditions. Increasing atmospheric anthropogenic aerosols played an important role in decreasing sunshine, especially for the past several decades. Weak sunshine years of the reconstruction matched well with years of major volcanic eruptions at interannual scale variations. Based on the significant cycles related to ENSO, PDO and AMO, sunshine variation in the southeastern Tibetan Plateau was possibly affected by the large-scale ocean-atmosphere circulation.

Acknowledgements

This study was jointly supported by Grants from the QYZDJ-SSW-DQC021, NSFC41630531, XDPB05, GJHZ1777, the CAS "Light of West China" Program, the Key Project of IEECAS (01) and the SKLLQG (020).

References

Bao, G., Liu, Y., Liu, N., 2012. A tree-ring-based reconstruction of the Yimin River annual runoff in the Hulun Buir region, Inner Mongolia, for the past 135 years. Chin. Sci. Bull. 57 (36), 4765–4775.

Bao, G., Liu, Y., Liu, N., Linderholm, H.W., 2015. Drought variability in eastern Mongolian Plateau and its linkages to the large-scale climate forcing. Clim. Dyn. 44 (3–4), 717–733.

Brown, J.M., 1968. The Photosynthetic Regime of some Southern Arizona Ponderosa Pine. University of Arizona, Tucson.

Che, H.Z., Shi, G.Y., Zhang, X.Y., Arimoto, R., Zhao, J.Q., Xu, L., Wang, B., Chen, Z.H., 2005. Analysis of 40 years of solar radiation data from China, 1961–2000. Geophys. Res. Lett. 32 (6), L06803. https://doi.org/10.1029/2004gl022322.

Chen, F., Yu, S.L., Yuan, Y.J., Wang, H.Q., Gagen, M., 2016. A tree-ring width based drought reconstruction for southeastern China, links to Pacific Ocean climate variability. Boreas 45 (2), 335–346.

Cho, H.K., Jeong, M.J., Kim, J., Kim, Y.J., 2003. Dependence of diffuse photosynthetically active solar irradiance on total optical depth. J. Geophys. Res.-Atmos. 108 (D9):4267. https://doi.org/10.1029/2002jd 002175.

Cook, E.R., Kairiukstis, L.A., 1990. Methods of Dendrochronology. Kluwer Academic Publishers, Dordrecht.

Cook, E.R., Meko, D.M., Stahle, D.W., Cleaveland, M.K., 1999. Drought reconstructions for the continental United States. J. Clim. 12 (4), 1145–1162.

Cook, E.R., Anchukaitis, K.J., Buckley, B.M., D'Arrigo, R.D., Jacoby, G.C., Wright, W.E., 2010. Asian monsoon failure and Megadrought during the last millennium. Science 328 (5977), 486–489.

Du, J., Bian, D., Hu, J., Liao, J., Zhou, M.J., 2007. Climatic change of sunshine duration and its influencing factors over Tibet during the last 35 years. Acta Geograph. Sin. 62 (5), 492–500.

Durbin, J., Watson, G.S., 1950. Testing for serial correlation in least squares regression: I. Biometrika 37 (3–4), 409–428.

Esper, J., Cook, E.R., Schweingruber, F.H., 2002. Low-frequency signals in long tree-ring chronologies for reconstructing past temperature variability. Science 295 (5563), 2250–2253.

Fan, Z.X., Brauning, A., Cao, K.F., 2008. Tree-ring based drought reconstruction in the central Hengduan Mountains region China. Since AD 1655. Int. J. Climatol. 28 (14), 1879–1887.

Fang, K.Y., Gou, X.H., Chen, F.H., Li, J.B., D'Arrigo, R., Cook, E., Yang, T., Davi, N., 2010. Reconstructed droughts for the southeastern Tibetan Plateau over the past 568 years and its linkages to the Pacific and Atlantic Ocean climate variability. Clim. Dyn. 35 (4), 577–585.

Farquhar, G.D., Roderick, M.L., 2003. Atmospheric science, Pinatubo, diffuse light, and the carbon cycle. Science 299 (5615), 1997–1998.

Frank, D., Esper, J., Cook, E.R., 2007. Adjustment for proxy number and coherence in a large-scale temperature reconstruction. Geophys. Res. Lett. 34 (16), L16709. https://doi.org/10.1029/2007gl030571.

Fritts, H.C., 1976. Tree Rings and Climate. Academic Press, New York.

Gagen, M., Zorita, E., McCarroll, D., Young, G.H.F., Grudd, H., Jalkanen, R., Loader, N.J., Robertson, I., Kirchhefer, A., 2011. Cloud response to summer temperatures in Fennoscandia over the last thousand years. Geophys. Res. Lett. 38, L05701. https://doi.org/10.1029/2010gl046216.

Gou, X.H., Yang, T., Gao, L.L., Deng, Y., Yang, M.X., Chen, F.H., 2013. A 457-year reconstruction of precipitation in the southeastern Qinghai-Tibet Plateau, China using tree-ring records. Chin. Sci. Bull. 58 (10), 1107–1114.

Griffin, D., Woodhouse, C.A., Meko, D.M., Stahle, D.W., Faulstich, H.L., Carrillo, C., Touchan, R., Castro, C.L., Leavitt, S.W., 2013. North American monsoon precipitation reconstructed from tree-ring latewood. Geophys. Res. Lett. 40 (5), 954–958.

Hafner, P., McCarroll, D., Robertson, I., Loader, N.J., Gagen, M., Young, G.H.F., Bale, R.J., Sonninen, E., Levanic, T., 2014. A 520 year record of summer sunshine for the eastern European alps based on stable carbon isotopes in larch tree rings. Clim. Dyn. 43 (3–4), 971–980.

Kaiser, D.P., Qian, Y., 2002. Decreasing trends in sunshine duration over China for 1954–1998, indication of increased haze pollution? Geophys. Res. Lett. 29 (21): 2042. https://doi.org/10.1029/2002gl016057.

Kanniah, K.D., Beringer, J., North, P., Hutley, L., 2012. Control of atmospheric particles on diffuse radiation and terrestrial plant productivity: a review. Prog. Phys. Geogr. 36 (2), 209–237.

Kelly, P.M., Jones, P.D., Robock, A., Briffa, K.R., 1998. The contribution of Hubert H. Lamb to the study of volcanic effects on climate. Weather 53 (7), 209–222.

Li, H.S., Ma, W.B., Lian, Y.W., Wang, X.L., Zhao, L., 2011. Global solar radiation estimation with sunshine duration in Tibet, China. Renew. Energy 36 (11), 3141–3145.

Li, R., Zhao, L., Ding, Y.J., Wu, T.H., Xiao, Y., Xin, Y.F., Sun, L.C., Hu, G.J., Zou, D.F., Jiao, Y.L., Qin, Y.H., 2012a. Variation characteristics of global radiation over the Tibetan Plateau during the past 40 years. J. Glaciol. Geocryol. 34 (6), 1319–1327.

Li, Z.X., Feng, Q., Zhang, W., He, Y.Q., Wang, X.F., Catto, N., An, W.L., Du, J.K., Chen, A.F., Liu, L., Hu, M., 2012b. Decreasing trend of sunshine hours and related driving forces in Southwestern China. Theor. Appl. Climatol. 109 (1–2), 305–321.

Li, J.B., Shi, J.F., Zhang, D.D., Yang, B., Fang, K.Y., Yue, P.H., 2017. Moisture increase in response to high-altitude warming evidenced by tree-rings on the southeastern Tibetan Plateau. Clim. Dyn. 48 (1–2), 649–660.

Liang, E.Y., Shao, X.M., Xu, Y., 2009. Tree-ring evidence of recent abnormal warming on the southeast Tibetan plateau. Theor. Appl. Climatol. 98 (1–2), 9–18.

Liang, E.Y., Wang, Y.F., Piao, S.L., Lu, X.M., Camarero, J.J., Zhu, H.F., Zhu, L.P., Ellison, A.M., Ciais, P., Penuelas, J., 2016. Species interactions slow warming-induced upward shifts of treelines on the Tibetan Plateau. Proc. Natl. Acad. Sci. USA 113 (16), 4380–4385.

Linderholm, H.W., Bjorklund, J., Seftigen, K., Gunnarson, B.E., Fuentes, M., 2015. Fennoscandia revisited, a spatially improved tree-ring reconstruction of summer temperatures for the last 900 years. Clim. Dyn. 45 (3–4), 933–947.

Liu, Y., An, Z.S., Linderholm, H.W., Chen, D.L., Song, H.M., Cai, Q.F., Sun, J.Y., Tian, H., 2009. Annual temperatures during the last 2485 years in the mid-eastern Tibetan Plateau inferred from tree rings. Sci. China Ser. D 52 (3), 348–359.

Liu, Y., Wang, Y.C., Li, Q., Song, H.M., Zhang, Y.H., Yuan, Z.L., Wang, Z.Y., 2015. A tree-ring-based June-September mean relative humidity reconstruction since 1837 from the Yiwulu Mountain region, China. Int. J. Climatol. 35 (7), 1301–1308.

Liu, Y., Cobb, K.M., Song, H.M., Li, Q., Li, C.Y., Nakatsuka, T., An, Z.S., Zhou, W.J., Cai, Q.F., Li, J.B., Leavitt, S.W., Sun, C.F., Mei, R.C., Shen, C.C., Chan, M.H., Sun, J.Y., Yan, L.B., Lei, Y., Ma, Y.Y., Li, X.X., Chen, D.L., Linderholm, H.W., 2017a. Recent enhancement of central Pacific El Nino variability relative to last eight centuries. Nat. Commun. 8, 15386. https://doi.org/10.1038/Ncomms15386.

Liu, Y., Liu, H., Song, H.M., Li, Q., Burr, G.S., Wang, L., Hu, S.L., 2017b. A monsoon-related 174-year relative humidity record from tree-ring $\delta^{18}O$ in the Yaoshan region, eastern central China. Sci. Total Environ. 593–594, 523–534.

Liu, Y., Zhang, X.J., Song, H.M., Cai, Q.F., Li, Q., Zhao, B.Y., Liu, H., Mei, R.C., 2017c. Tree-ring-width-based PDSI reconstruction for central Inner Mongolia, China over the past 333 years. Clim. Dyn. 48 (3–4), 867–879.

Loader, N.J., Young, G.H.F., Grudd, H., McCarroll, D., 2013. Stable carbon isotopes from Tornetrask, northern Sweden provide a millennial length reconstruction of summer sunshine and its relationship to Arctic circulation. Quat. Sci. Rev. 62, 97–113.

Mann, M.E., Zhang, Z.H., Hughes, M.K., Bradley, R.S., Miller, S.K., Rutherford, S., Ni, F.B., 2008. Proxy-based reconstructions of hemispheric and global surface temperature variations over the past two millennia. P. Natl. Acad. Sci. USA 105 (36), 13252–13257.

Melvin, T.M., Briffa, K.R., 2008. A "signal-free" approach to dendroclimatic standardisation. Dendrochronologia 26 (2), 71–86.

Mohtadi, M., Prange, M., Steinke, S., 2016. Palaeoclimatic insights into forcing and response of monsoon rainfall. Nature 533 (7602), 191–199.

Osborn, T.J., Briffa, K.R., Jones, P.D., 1997. Adjusting variance for sample-size in tree-ring chronologies and other regional-mean time-series. Dendrochronologia 15, 89–99.

Pinker, R.T., Zhang, B., Dutton, E.G., 2005. Do satellites detect trends in surface solar radiation? Science 308 (5723), 850–854.

Poljansek, S., Ceglar, A., Levanic, T., 2013. Long-term summer sunshine/moisture stress reconstruction from tree-ring widths from Bosnia and Herzegovina. Clim. Past 9 (1), 27–40.

Popa, I., Kern, Z., 2009. Long-term summer temperature reconstruction inferred from tree-ring records from the Eastern Carpathians. Clim. Dyn. 32 (7–8), 1107–1117.

Pumijumnong, N., Eckstein, D., Nathsuda, P., Dieter, E., 2011. Reconstruction of pre-monsoon weather conditions in northwestern Thailand from the tree-ring widths of *Pinus merkusii* and *Pinus kesiya*. Trees 25 (1), 125–132.

Qian, Y., Kaiser, D.P., Leung, L.R., Xu, M., 2006. More frequent cloud-free sky and less surface solar radiation in China from 1955 to 2000. Geophys. Res. Lett. 33 (1), L01812. https://doi.org/10.1029/2005gl024586.

Qian, Y., Wang, W.G., Leung, L.R., Kaiser, D.P., 2007. Variability of solar radiation under cloud-free skies in China, the role of aerosols. Geophys. Res. Lett. 34 (12), L12804. https://doi.org/10.1029/2006gl028800.

Robock, A., 2000. Volcanic eruptions and climate. Rev. Geophys. 38 (2), 191–219.

Shao, X.M., Huang, L., Liu, H.B., Liang, E.Y., Fang, X.Q., Wang, L.L., 2005. Reconstruction of precipitation variation from tree rings in recent 1000 years in Delingha, Qinghai. Sci. Chin. Ser. D 48 (7), 939–949.

Shi, C.M., Masson-Delmotte, V., Daux, V., Li, Z.S., Carre, M., Moore, J.C., 2015. Unprecedented recent warming rate and temperature variability over the east Tibetan Plateau inferred from Alpine treeline dendrochronology. Clim. Dyn. 45 (5–6), 1367–1380.

Siebert, L., Simkin, T., 2013. Volcanoes of the World: An Illustrated Catalog of Holocene Volcanoes and their Eruptions. Smithsonian Institution, Global Volcanism Program Digital Information Series, GVP-3. URL:. http://www.volcano.si.edu.

Stahle, D.W., Cleaveland, M.K., Cerveny, R.S., 1991. Tree-ring reconstructed sunshine duration over Central USA. Int. J. Climatol. 11 (3), 285–295.

Stanhill, G., Cohen, S., 2001. Global dimming: a review of the evidence for a widespread and significant reduction in global radiation with discussion of its probable causes and possible agricultural consequences. Agric. For. Meteorol. 107 (4), 255–278.

Thomas, A., 2000. Spatial and temporal characteristics of potential evapotranspiration trends over China. Int. J. Climatol. 20 (4), 381–396.

Thomson, D.J., 1982. Spectrum estimation and harmonic-analysis. Proc. IEEE 70 (9), 1055–1096.

Wigley, T.M.L., Briffa, K.R., Jones, P.D., 1984. On the average value of correlated time-series, with applications in dendroclimatology and hydrometeorology. J. Clim. Appl. Meteorol. 23 (2), 201–213.

Wilson, R., Anchukaitis, K., Briffa, K.R., Buntgen, U., Cook, E., D'Arrigo, R., Davi, N., Esper, J., Frank, D., Gunnarson, B., Hegerl, G., Helama, S., Klesse, S., Krusic, P.J., Linderholm, H.W., Myglan, V., Osborn, T.J., Rydval, M., Schneider, L., Schurer, A., Wiles, G., Zhang, P., Zorita, E., 2016. Last millennium northern hemisphere summer temperatures from tree rings, part I, the long term context. Quat. Sci. Rev. 134, 1–18.

Wu, Z.H., Huang, N.E., Chen, X.Y., 2009. The multi-dimensional ensemble empirical mode decomposition method. Adv. Adap. Data Anal. 1 (3), 339–372.

Xia, X.G., 2010. Spatiotemporal changes in sunshine duration and cloud amount as well as their relationship in China during 1954–2005. J. Geophys. Res-Atmos. 115, D00k06. https://doi.org/10.1029/2009jd012879.

Yang, Y.H., Zhao, N., Hao, X.H., Li, C.Q., 2009. Decreasing trend of sunshine hours and related driving forces in North China. Theor. Appl. Climatol. 97 (1–2), 91–98.

Yang, X.M., An, W.L., Zhang, W., Chang, L., Wang, Y.M., 2012. Variation of sunshine hours and related driving forces in southwestern China. J. Lanzhou Univ. (Nat. Sci.) 48 (5), 52–60.

Yang, B., Qin, C., Wang, J.L., He, M.H., Melvin, T.M., Osborn, T.J., Briffa, K.R., 2014. A 3,500-year tree-ring record of annual precipitation on the northeastern Tibetan Plateau. P. Natl. Acad. Sci. USA 111 (8), 2903–2908.

Yu, H.Y., Liu, S.H., Zhao, N., Yu, Y.T., Yu, L.P., Cao, H.W., 2011. Variation characteristics of the sunshine duration and its relationships with temperature,wind speed,and precipitation over recent 59 years in China. Clim. Environ. Res. 16 (3), 389–398.

Zhang, Z.H., 2015. Tree-rings, a key ecological indicator of environment and climate change. Ecol. Indic. 51, 107–116.

Zhang, T.W., Yuan, Y.J., Wei, W.S., Yu, S.L., Zhang, R.B., Chen, F., Shang, H.M., Qin, L., 2014. A tree-ring based precipitation reconstruction for the Mohe region in the northern Greater Higgnan Mountains, China, since AD 1724. Quat. Res. 82 (1), 14–21.

Zhang, Q.B., Evans, M.N., Lyu, L.X., 2015. Moisture dipole over the Tibetan Plateau during the past five and a half centuries. Nat. Commun. 6, 8062. https://doi.org/10.1038/Ncomms9062.

Zhao, J., Chen, C.K., 1999. Geography of China. Higher Education Press, Beijing.

Zheng, X.B., Kang, W.M., Zhao, T.L., Luo, Y.X., Duan, C.C., Chen, J., 2008. Long-term trends in sunshine duration over Yunnan-Guizhou Plateau in Southwest China for 1961–2005. Geophys. Res. Lett. 35 (15), L15707. https://doi.org/10.1029/2008gl034482.

Zhu, H.F., Shao, X.M., Yin, Z.Y., Xu, P., Xu, Y., Tian, H., 2011. August temperature variability in the southeastern Tibetan Plateau since AD 1385 inferred from tree rings. Palaeogeogr. Palaeocl. 305 (1–4), 84–92.